

3D Ln^{III}-MOFs: displaying slow magnetic relaxation and highly sensitive luminescent sensing of alkylamines

Hong Huang^a, Wei Gao^{*a}, Xiu-Mei Zhang^{*ab}, Ai-Mei Zhou^a and Jie-Ping Liu^a

^aCollege of Chemistry and Materials Science, Huaibei Normal University, Anhui 235000, China

^bState Key Laboratory of Coordination Chemistry, Nanjing University, Nanjing, China

Table S1 Selected bond lengths [Å] and angles [°] for Pr-MOF (**1**).

Pr-MOF (1)			
Pr1-O6A	2.362(3)	Pr1-O3B	2.399(3)
Pr1-O4C	2.410(3)	Pr1-O11	2.457(4)
Pr1-O10	2.497(4)	Pr1-O2	2.539(3)
Pr1-O1	2.539(3)	Pr1-O9	2.549(3)
O6A-Pr1-O3B	151.37(13)	O6A-Pr1-O4C	84.79(13)
O3B-Pr1-O4C	109.63(12)	O6A-Pr1-O11	78.06(15)
O3B-Pr1-O11	76.16(15)	O4C-Pr1-O11	144.42(14)
O6A-Pr1-O10	98.2(2)	O3B-Pr1-O10	84.26(19)
O4C-Pr1-O10	144.59(16)	O11-Pr1-O10	69.47(18)
O6A-Pr1-O2	129.97(11)	O3B-Pr1-O2	78.47(11)
O4C-Pr1-O2	74.78(11)	O11-Pr1-O2	139.11(13)
O10-Pr1-O2	76.57(17)	O6A-Pr1-O1	79.67(10)
O3B-Pr1-O1	126.98(12)	O4C-Pr1-O1	76.36(11)
O11-Pr1-O1	129.43(13)	O10-Pr1-O1	69.61(15)
O2-Pr1-O1	51.50(9)	O6A-Pr1-O9	76.96(12)
O3B-Pr1-O9	84.35(13)	O4C-Pr1-O9	71.24(12)

O11-Pr1-O9	74.61(14)	O10-Pr1-O9	143.95(16)
O2-Pr1-O9	133.75(10)	O1-Pr1-O9	141.34(12)

A x-1/2,y-1/2,-z+1/2; B x-1/2,-y+1/2,-z+1; C -x+5/2,y-1/2,z.

Table S2 Selected bond lengths [\AA] and angles [$^\circ$] for Sm-MOF (**2**).

Sm-MOF (2)			
Sm1-O6A	2.316(4)	Sm1-O4B	2.348(4)
Sm1-O3C	2.350(4)	Sm1-O11	2.411(5)
Sm1-O10	2.439(5)	Sm1-O2	2.494(4)
Sm1-O9	2.498(5)	Sm1-O1	2.498(4)
O6A-Sm1-O4B	84.99(16)	O6A-Sm1-O3C	151.30(15)
O4B-Sm1-O3C	108.32(16)	O6A-Sm1-O11	78.27(18)
O4B-Sm1-O11	144.55(18)	O3C-Sm1-O11	76.49(17)
O6A-Sm1-O10	97.3(2)	O4B-Sm1-O10	145.01(17)
O3C-Sm1-O10	86.2(2)	O11-Sm1-O10	68.85(19)
O6A-Sm1-O2	130.47(14)	O4B-Sm1-O2	74.67(15)
O3C-Sm1-O2	78.16(14)	O11-Sm1-O2	138.85(17)
O10-Sm1-O2	77.65(17)	O6A-Sm1-O9	78.07(15)
O4B-Sm1-O9	71.68(15))	O3C-Sm1-O9	82.17(16)
O11-Sm1-O9	74.37(17)	O10-Sm1-O9	143.07(17)
O2-Sm1-O9	132.90(14)	O6A-Sm1-O1	79.19(14)
O4B-Sm1-O1	76.10(15)	O3C-Sm1-O1	128.07(14)
O11-Sm1-O1	129.62(16)	O10-Sm1-O1	70.13(17)
O2-Sm1-O1	52.43(12)	O9-Sm1-O1	141.79(15)

A x-1/2,y-1/2,-z+1/2; B -x+5/2,y-1/2,z; C x-1/2,-y+1/2,-z+1.

Table S3 Selected bond lengths [\AA] and angles [$^\circ$] for Eu-MOF (**3**).

Eu-MOF (3)			

Eu1-O6A	2.301(3)	Eu1-O3B	2.333(3)
Eu1-O4C	2.335(3)	Eu1-O11	2.403(4)
Eu1-O10	2.425(4)	Eu1-O2	2.477(3)
Eu1-O1	2.487(3)	Eu1-O9	2.491(3)
O6A-Eu1-O3B	151.37(12)	O6A-Eu1-O4C	84.89(13)
O3B-Eu1-O4C	108.12(12)	O6A-Eu1-O11	78.53(15)
O3B-Eu1-O11	76.37(14)	O4C-Eu1-O11	144.40(14)
O6A-Eu1-O10	96.32(15)	O3B-Eu1-O10	87.50(15)
O4C-Eu1-O10	144.58(14)	O11-Eu1-O10	69.22(15)
O6A-Eu1-O2	130.74(11)	O3B-Eu1-O2	77.83(11)
O4C-Eu1-O2	74.84(12)	O11-Eu1-O2	138.64(13)
O10-Eu1-O2	77.92(14)	O6A-Eu1-O1	79.23(11)
O3B-Eu1-O1	128.04(11)	O4C-Eu1-O1	76.22(11)
O11-Eu1-O1	129.84(13)	O10-Eu1-O1	69.32(13)
O2-Eu1-O1	52.69(9)	O6A-Eu1-O9	78.18(11)
O3B-Eu1-O9	81.94(12)	O4C-Eu1-O9	71.59(11)
O11-Eu1-O9	74.27(13)	O10-Eu1-O9	143.43(14)
O2-Eu1-O9	132.65(10)	O1-Eu1-O9	141.92(11)

A x-1/2,y-1/2,-z+1/2; B x-1/2,-y+1/2,-z+1; C -x+5/2,y-1/2,z.

Table S4 Selected bond lengths [Å] and angles [°] for Gd-MOF (**4**).

Gd-MOF (4)			
Gd1-O6A	2.291(4)	Gd1-O4B	2.314(4)
Gd1-O3C	2.322(4)	Gd1-O11	2.385(6)
Gd1-O10	2.398(5)	Gd1-O2	2.468(4)
Gd1-O1	2.473(4)	Gd1-O9	2.480(4)
O6A-Gd1-O4B	85.17(16)	O6A-Gd1-O3C	150.83(16)
O4B-Gd1-O3C	107.28(15)	O6A-Gd1-O11	77.6(2)
O4B-Gd1-O11	144.00(17)	O3C-Gd1-O11	77.20(19)

O6A-Gd1-O10	98.9(2)	O4B-Gd1-O10	145.45(19)
O3C-Gd1-O10	85.7(2)	O11-Gd1-O10	69.3(2)
O6A-Gd1-O2	131.43(14)	O4B-Gd1-O2	75.00(15)
O(3)C-Gd1-O2	77.73(14)	O11-Gd1-O2	138.95(16)
O10-Gd1-O2	76.90(19)	O6A-Gd1-O1	79.60(14)
O4B-Gd1-O1	76.51(15)	O3C-Gd1-O1	128.44(14)
O11-Gd1-O1	129.53(17)	O10-Gd1-O1	70.63(18)
O2-Gd1-O1	53.00(11)	O6A-Gd1-O9	78.50(14)
O4B-Gd1-O9	71.54(15)	O3C-Gd1-O9	80.68(15)
O11-Gd1-O9	74.15(17)	O10-Gd1-O9	142.98(19)
O2-Gd1-O9	132.16(13)	O1-Gd1-O9	142.40(14)

A x-1/2,y-1/2,-z+1/2; B -x+5/2,y-1/2,z; C x-1/2,-y+1/2,-z+1.

Table S5 Selected bond lengths [\AA] and angles [°] for Dy-MOF (5).

Dy-MOF (5)			
Dy1-O6A	2.278(4)	Dy1-O3B	2.298(4)
Dy1-O4C	2.305(4)	Dy1-O11	2.388(5)
Dy1-O10	2.392(5)	Dy1-O2	2.457(4)
Dy1-O9	2.458(4)	Dy1-O1	2.467(4)
O6A-Dy1-O3B	151.69(16)	O6A-Dy1-O4C	85.13(15)
O3B-Dy1-O4C	107.48(14)	O6A-Dy1-O11	78.54(18)
O3B-Dy1-O11	76.79(17)	O4C-Dy1-O11	144.53(16)
O6A-Dy1-O10	96.16(19)	O3B-Dy1-O10	87.99(17)
O4C-Dy1-O10	144.36(18)	O11-Dy1-O10	69.36(19)
O6A-Dy1-O2	130.98(14)	O3B-Dy1-O2	77.28(13)
O4C-Dy1-O2	74.96(14)	O11-Dy1-O2	138.31(15)
O10-Dy1-O2	77.65(19)	O6A-Dy1-O9	79.18(14)
O3B-Dy1-O9	80.89(15)	O4C-Dy1-O9	72.00(15)
O11-Dy1-O9	74.11(16)	O10-Dy1-O9	143.35(19)

O2-Dy1-O9	132.25(13)	O6A-Dy1-O1	78.60(13)
O3B-Dy1-O1	128.46(14)	O4C-Dy1-O1	76.28(14)
O11-Dy1-O1	129.53(15)	O10-Dy1-O1	69.16(17)
O2-Dy1-O1	53.49(11)	O9-Dy1-O1	142.45(15)

A x-1/2,y-1/2,-z+1/2; B x-1/2,-y+1/2,-z+1; C -x+5/2,y-1/2,z.

Table S6 Selected bond lengths [Å] and angles [°] for Ho-MOF (**6**).

Ho-MOF (6)			
Ho1-O6A	2.264(3)	Ho1-O4B	2.280(3)
Ho1-O3C	2.288(3)	Ho1-O11	2.365(4)
Ho1-O10	2.379(4)	Ho1-O1	2.447(3)
Ho1-O2	2.449(3)	Ho1-O9	2.450(4)
O6A-Ho1-O4B	85.15(13)	O6A-Ho1-O3C	151.13(13)
O4B-Ho1-O3C	106.86(12)	O6A-Ho1-O11	77.90(15)
O4B-Ho1-O11	144.05(14)	O3C-Ho1-O11	77.33(14)
O6A-Ho1-O10	98.25(17)	O4B-Ho1-O10	145.60(14)
O3C-Ho1-O10	86.51(17)	O11-Ho1-O10	69.02(15)
O6A-Ho1-O1	78.81(11)	O4B-Ho1-O1	76.40(12)
O3C-Ho1-O1	129.06(11)	O11-Ho1-O1	129.45(13)
O10-Ho1-O1	70.82(14)	O6A-Ho1-O2	131.53(11)
O4B-Ho1-O2	75.18(12)	O3C-Ho1-O2	77.33(11)
O11-Ho1-O2	138.59(13)	O10-Ho1-O2	77.25(15)
O1-Ho1-O2	53.83(9)	O6A-Ho1-O9	79.19(12)
O4B-Ho1-O9	71.95(13)	O3C-Ho1-O9	79.86(12)
O11-Ho1-O9	73.84(14)	O10-Ho1-O9	142.41(15)
O1-Ho1-O9	142.62(12)	O2-Ho1-O9	132.00(11)

A x-1/2,y-1/2,-z+1/2; B -x+5/2,y-1/2,z; C x-1/2,-y+1/2,-z+1.

Table S7 Hydrogen bond lengths (\AA) and angles ($^\circ$) for Dy-MOF (**5**)^a.

D	A[Transformation]	d(D-H)	d(H \cdots A)	d(D \cdots A)	\angle (DHA)
O9	O5 [x-1/2, y-1/2, -z+1/2]	0.733(8)	2.158(8)	2.778(6)	140.2(5)
O9	O2 [2-x, -y, 1-z; H 5/2-x]	1.045(7)	1.894(6)	2.827 (6)	150.6(9)

^a D, donor; A, acceptor.

Table S8 A comparison between MOF-based luminescent sensors sensing towards alkylamines.

Analyte	MOF	Solution	Detection Limit	K_{sv} (M^{-1})	Ref.
TEA	$[\text{Zr}_6\text{O}_4(\text{OH})_4(\text{dmbpydc})_4(\text{mbpydc})_{1.3}(\text{bpydc})_{0.7}] \cdot (\text{OTf})_{9.3}$	EtOH	----	4.91×10^3 4.51×10^3	42
EDA	$[\text{Tb}_2(\text{csal})_6(\text{H}_2\text{O})_4] \cdot 4\text{H}_2\text{O}$	DMF	----	5.583×10^3	44
TEA	$[\text{Tb}_2(\text{csal})_6(\text{H}_2\text{O})_4] \cdot 4\text{H}_2\text{O}$	DMF	----	2.698×10^3	44
EDA	$[\text{Cd}_2\text{Cl}(\text{m-bpybdc})_2(\text{H}_2\text{O})_4](\text{NO}_3)_3 \cdot 7\text{H}_2\text{O}$	air	----	----	43
EDA	Mg-NDI	EtOH	----	8.4×10^2	45
TEA	Mg-NDI	EtOH	----	6.6	45

dmbpydc = 1,1'-dimethyl-2,2'-bipyridine-5,5'-dicarboxylate;

mbpydc = 1-methyl-2,2'-bipyridine-5,5'-dicarboxylate;

Bpydc = 2,2'-bipyridyl-5,5'-dicarboxylate;

TfOMe = trifluoromethanesulfonate;

Hcsal = 4-chlorosalicylic acid;

m-bpybdc = 4,4'-bipyridinium-1,1'-bis(phenylene-3-carboxylate);

NDI = naphthalenediimide.

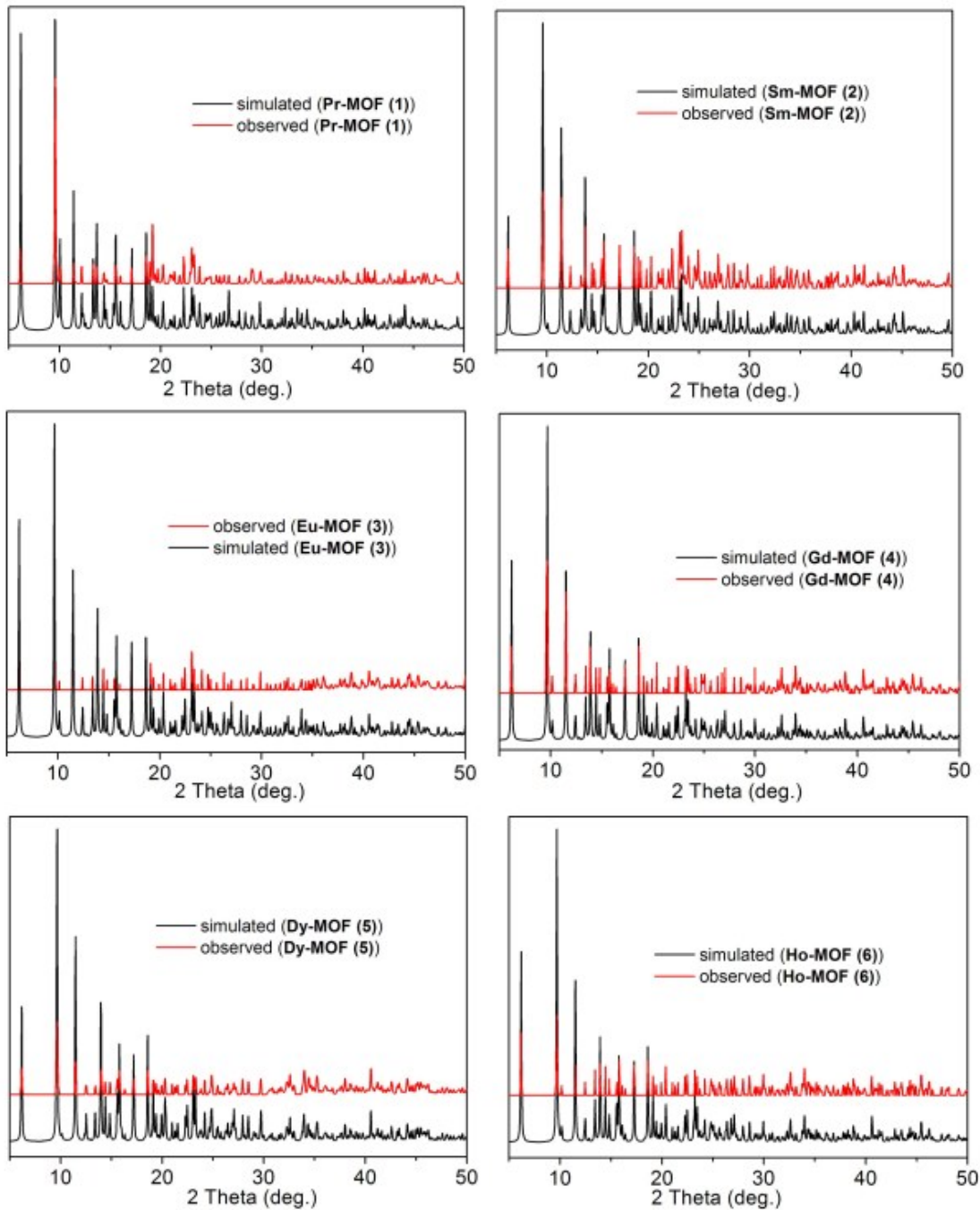


Fig. S1 Powder X-ray diffraction patterns of 1-6.

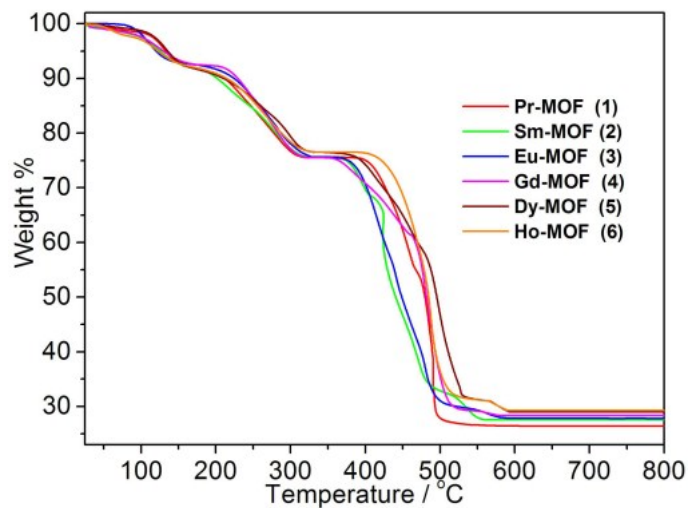


Fig. S2 TGA curves for 1-6.

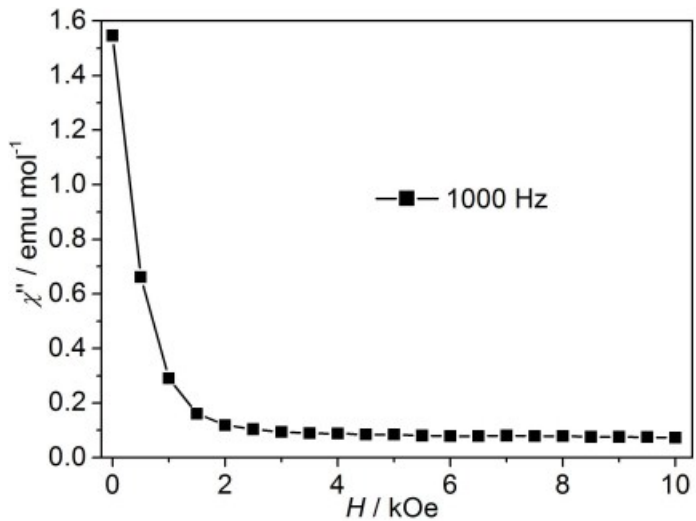


Fig. S3 The out-of-phase (χ'') ac susceptibility for Dy-MOF (5) (2 K, f = 1000 Hz) under the applied static field from 0-10 kOe.

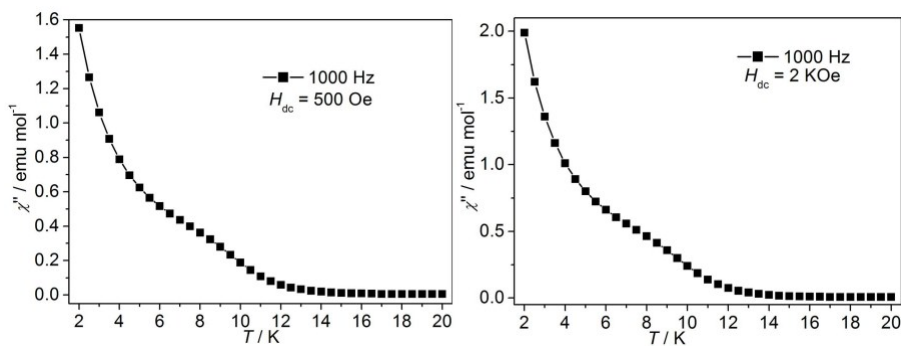


Fig. S4 Temperature dependence of the out-of-phase ac susceptibility for Dy-MOF (5) under 500 Oe (left) and 2000 Oe (right) dc field.

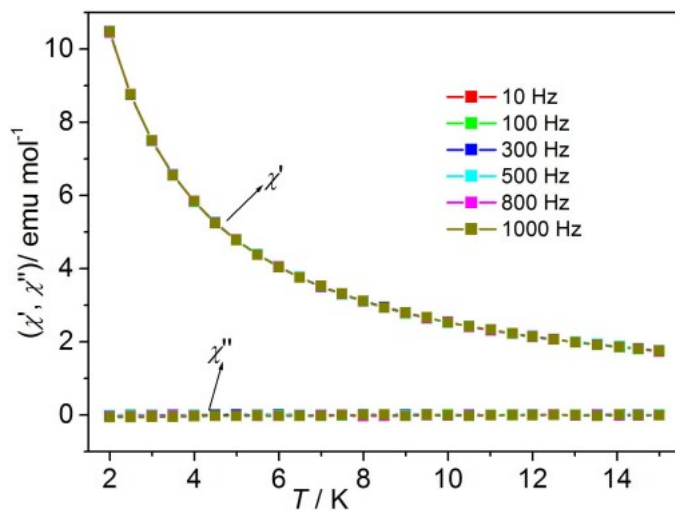


Fig. S5 The ac susceptibilities of Ho-MOF (**6**) at 2 K under $Hdc = 0$ Oe.

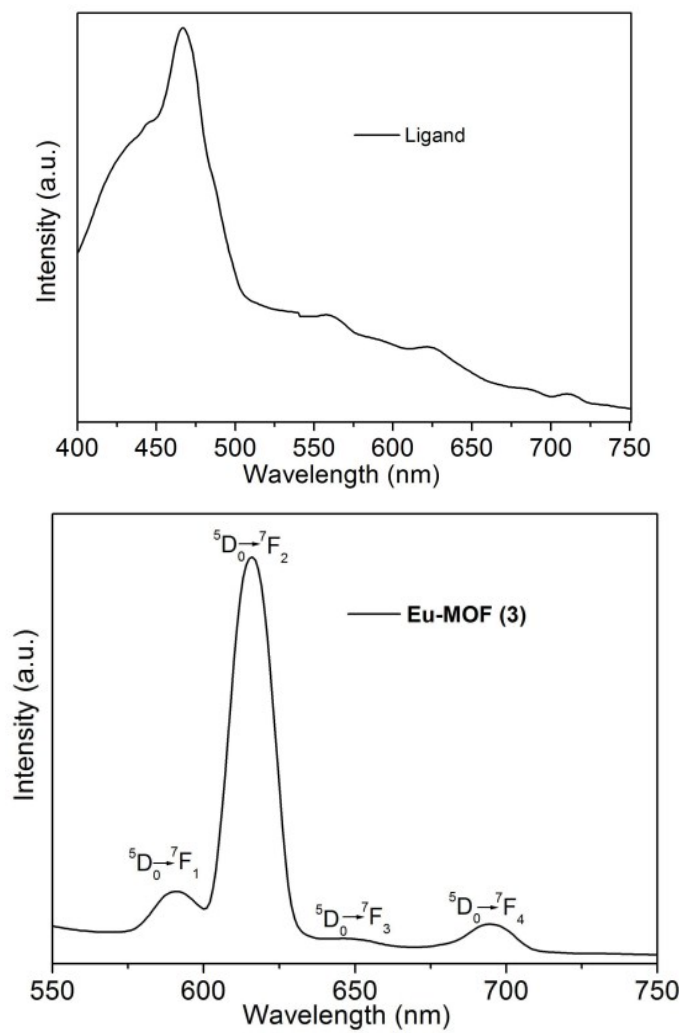


Fig. S6 Solid sample emission spectra of the H_3L ligand (top) and Eu-MOF (**3**) (bottom) at 298 K.

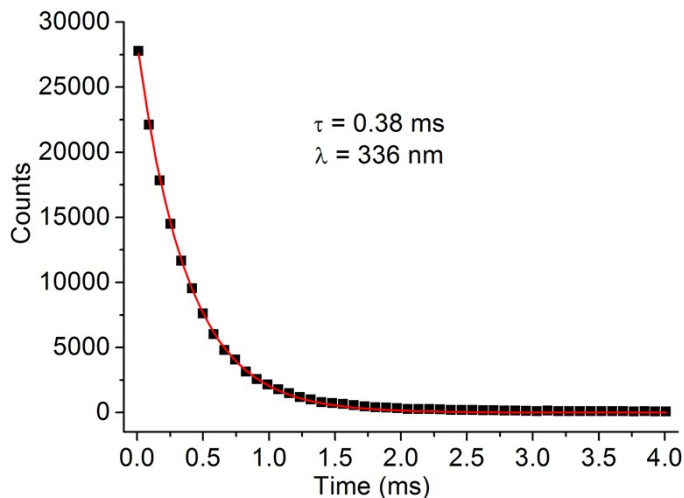


Fig. S7 The fluorescence decay curve for Eu-MOF (3) ($\lambda_{\text{ex}} = 336 \text{ nm}$) in solid state at 298 K.

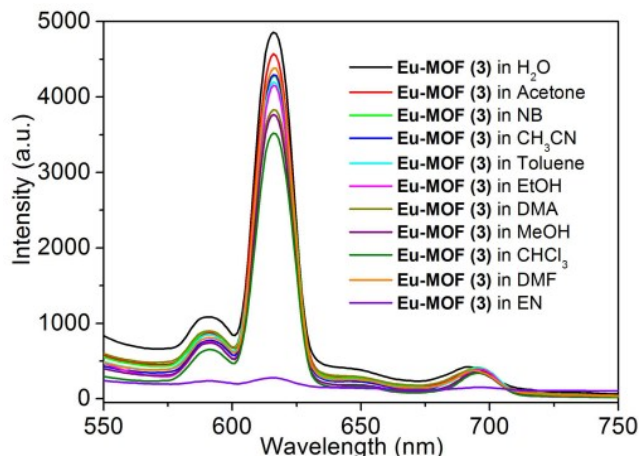


Fig. S8 Luminescent spectra of Eu-MOF (3) dispersed in different small molecules.

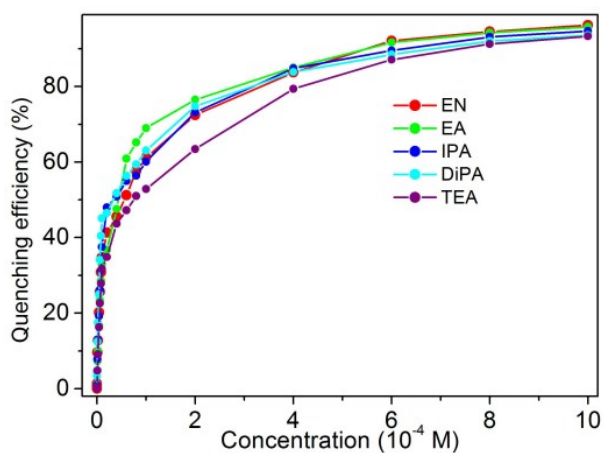


Fig. S9 Quenching efficiency of Eu-MOF (3) dispersed in aqueous solution with the addition of alkylamines (EN, EA, IPA, DiPA and TEA).

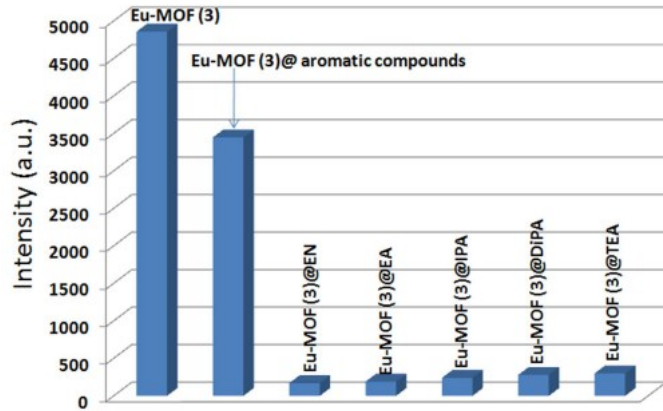


Fig. S10 Luminescent intensities of the ${}^5D_0 \rightarrow {}^7F_2$ emission of dispersed in aqueous solutions of mixed aromatic compounds without or with alkylamines (EN, EA, IPA, DiPA and TEA).

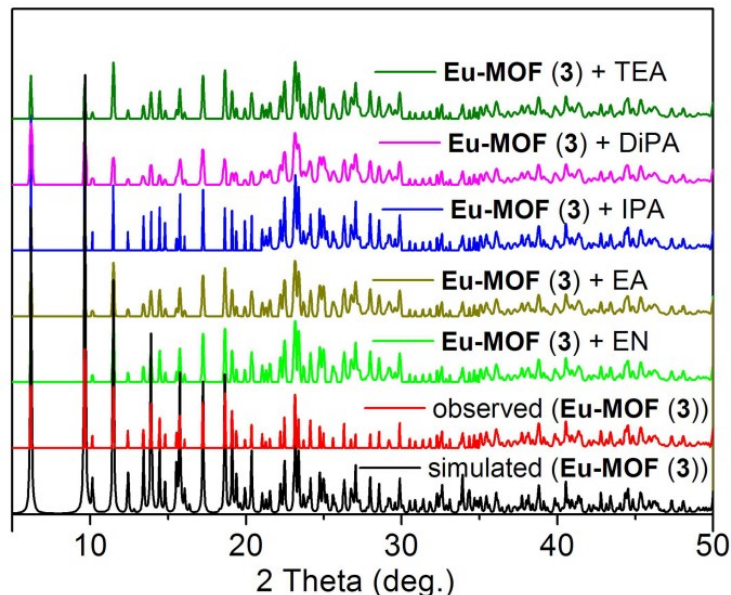


Fig. S11 Power X-ray diffraction patterns of Eu-MOF (3)@ alkylamines (EN, EA, IPA, DiPA and TEA).

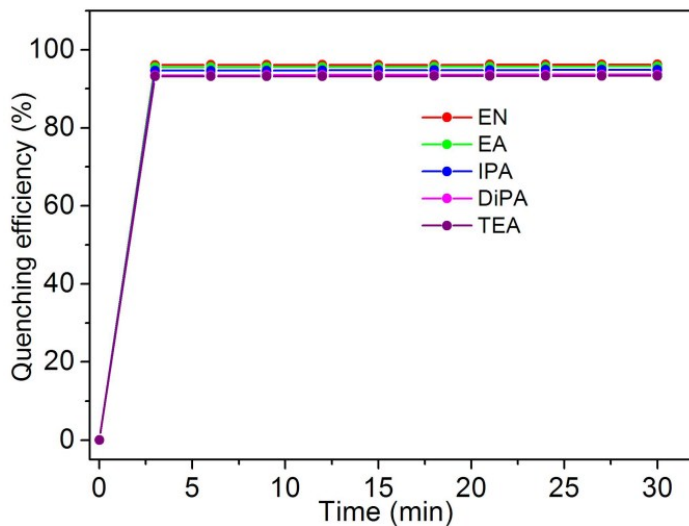


Fig. S12 Time dependence of the quenching efficiency at 616 nm (excited at 336 nm) of the aqueous dispersions of Eu-MOF (3) upon addition of alkylamines (EN, EA, IPA, DiPA and TEA, 1 mM).

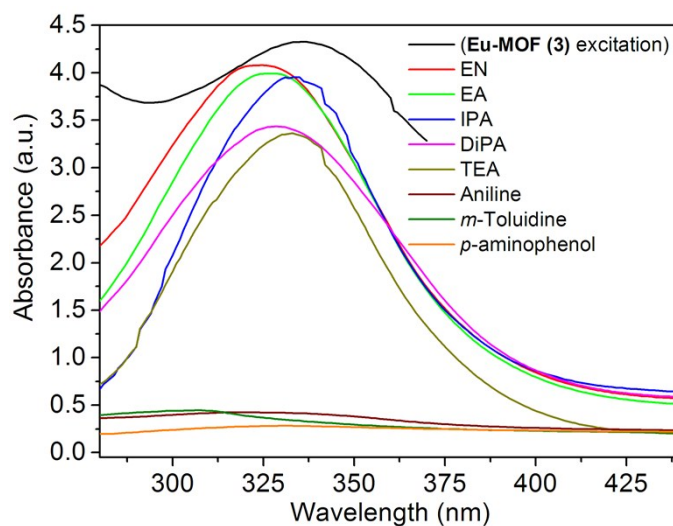


Fig. S13 The UV-Vis absorption spectrum of aqueous solutions of different testing amine compounds (EN, EA, IPA, DiPA, TEA, Aniline, *m*-Toluidine and *p*-aminophenol) and the excitation of Eu-MOF (3).